On interfacial instability as a cause of transverse subcritical bed forms

Jeremy G. Venditti,[1] Michael Church,[2] and Sean J. Bennett[3]

[1] Recent experimental results suggest there are at least two distinct bed form initiation processes. Bed forms may be generated from local bed defects that are propagated down and across stream by flow separation processes when sediment transport is patchy and sporadic. Alternatively, bed form development may occur over the whole bed at once when sediment transport is general and widespread. Herein, we critically test a simple model for this latter bed form initiation mode that was originally presented by H.-K. Liu in 1957 but not tested because of the complex nature of the measurements required. The theory is based on the idea that a moving sand bed might be likened to a dense fluid and that a hydrodynamic instability develops at the interface between the sediment transport layer and the near-bed fluid, leading to the organization of the transport system into laterally extended, discrete bed forms. Our predicted initial bed form lengths are within 10% of the lengths observed in a series of flume experiments, suggesting that transverse waveforms on sand beds sheared by unidirectional currents can be initiated as an interfacial hydrodynamic instability of Kelvin-Helmholtz type when the current is sufficiently vigorous to produce general sediment movement, that is, to create a sediment transport layer that acts as a pseudofluid with density composed of solid and fluid components.

1. Introduction

[2] In addition to being a stunning visual manifestation of apparent order in geological processes, sedimentary bed forms represent primary roughness elements that are known to significantly modulate hydraulic processes and sediment transport in a variety of geophysical flows. Bed forms are also used to infer the magnitude and frequency of paleo-flows. Understanding their origin, development and dynamics is critical to understanding the flows that give rise to them. Yet, in spite of their importance for understanding both active Earth processes and the geological record, the work of more than a century has not settled the question of their origin [*Raudkivi*, 1997]. Ideas about the initiation of the dominant subcritical flow-transverse bed forms (ripples, dunes, in general, "sand waves"; see *Allen* [1982] and *Ashley* [1990] for reviews on the vexed question of terminology) fall into four general categories: (1) the formation and propagation of a bed defect, (2) kinematic wave formation or other interference phenomena in the granular transport, (3) the imposition of an amplifying perturbation

onto the labile bed, and (4) the generation of an interfacial instability at the water-sediment interface.

[3] The idea that bed forms originate from boundary defects, either preexisting ones or ones imposed by the flow, goes back to the turn of the 20th century and constitutes the oldest attempt to explain their occurrence [see *Allen*, 1982]. Growth of transverse bed forms from an initial mound or hollow has been demonstrated experimentally by *U.S. Army Corps of Engineers* [1935], *Rathbun and Guy* [1967], *Southard and Dingler* [1971], *Leeder* [1980] and *Best* [1992], and is not hard to observe in natural water courses, where sand waves often are seen to propagate downstream from an obstacle such as a bank protuberance, wood debris, or an isolated stone (showing that the initiating perturbation need not be part of the deformable bed). *Raudkivi* [1963, 1966] proposed, after a series of experiments, that flow separation over the defect and the characteristics of the separated flow control wave propagation by controlling the convergence and divergence of flow, consequently the erosion and deposition of sediment.

[4] The process was further analyzed by *Grass* [1970] and by *Williams and Kemp* [1971], who proposed that the initial defects may be irregularities in the granular bed, only one or a few grain diameters in height, created by the entrainment and transport of sediment by coherent turbulent flow structures. In particular, microturbulent sweeps have been associated with the production of flow-parallel ridges (sand streaks) which flare at their downstream ends where the sweep lifts off, creating small sediment accumulations

[1]Department of Earth and Planetary Sciences, University of California, Berkeley, California, USA.
[2]Department of Geography, University of British Columbia, Vancouver, British Columbia, Canada.
[3]Department of Geography, State University of New York at Buffalo, Buffalo, New York, USA.

that constitute bed defects. Flow separation over the defects is said to enhance turbulence intensity, erosion and sediment transport in the lee of the defect. However, a fall in turbulence intensity downstream from the reattachment point leads to sediment deposition and propagation of the defect. The process and supporting evidence have been described in detail by *Allen* [1982], *Gyr and Schmid* [1989], and *Best* [1992] following descriptions of micro-turbulent structures elaborated in the fluid mechanics literature [e.g., *Kline et al.*, 1967; *Kim et al.*, 1971]. However, *Allen* [1982] pointed out the gross spatial discordance between the scale of these structures, of order D (grain diameter), and even small transverse bed forms. Turbulent flow is, furthermore, highly disorganized spatially, and is characterized by the generation of short-lived eddy structures by nonperiodic and probably nonlinear processes [see *Nezu and Nakagawa*, 1993; *Ashworth et al.*, 1996]. In contrast, the evolution of the highly organized bed structure is slow, since significant volumes of sediment must be moved in a consistent way. It is not clear how slowly evolving bed forms can result from random turbulent structures unless the turbulence becomes phase locked. There is evidence for such phase locking [*Best*, 1992] over sand streaks, but that appears rather to emphasize the ridge structure than to generate transverse features. In any case, *Kuru et al.* [1995] and *Coleman and Eling* [2000] have recently reported the development of bed forms in laminar flows. Indeed, the former authors found no significant change in bed form initiation across the transition to turbulent flow. Although turbulent flow structures certainly promote the initiation and maintenance of sediment transport, it is not clear that they control the macroscale organization of the bed.

[5] The notion of grain-grain interference leading to kinematic clumping was raised by *Bagnold* [1935] in relation to aeolian ballistic ripples. The theory was developed by *Lighthill and Witham* [1955a, 1955b] and advocated by *Langbein and Leopold* [1968] and by *Costello* [1974] for current bed forms in water. The idea is consistent with turbulent modulation of flow and transport along streamlines and the phenomenon could conceivably form the grain clumps attributed above to the liftoff of micro-turbulent sweeps, but it has not been shown that this mechanism can, in general, give rise to laterally extended features unless some larger-scale transverse flow structure controls the effective variations in transport and kinematic interference. It could, however, be particularly effective in saltating transport (Bagnold's original concept) due to the imposition of a characteristic grain step length.

[6] The concept of amplifying perturbations is the most widely accepted basis for analyzing transverse bed forms today. It is based on the observation that an initial perturbation will develop if the sediment transport falls out of phase with some flow property that controls the transport. For example, sediment inertia may dictate that the adjustment of transport lags the variation in fluid shear stress (or power) [*Bagnold*, 1956; *Reynolds*, 1965]. Variations in shear stress are supposed to arise, in the first instance, from well-known variations in the turbulent velocity profile over the rough bed [e.g., *Laufer*, 1951; *Klebanoff*, 1955]. Given the phase shift, sediment transport and deposition lead to a topographic wave that is amplified as its presence comes to

modulate the flow over it, which really amounts to impressing an initial defect onto the bed from the flow. What ultimately are the dominant stable waveforms has been investigated by stability analyses. This approach was proposed by F.M. Exner in the 1920s [see *Leliavsky*, 1955] and developed by *Anderson* [1953]. Modern work, including analyses by *Kennedy* [1963, 1969], *Reynolds* [1965], *Engelund* [1970], *Smith* [1970], *Fredsøe* [1974], *Parker* [1975], and *Richards* [1980], leads to stability diagrams for subcritical (dune) and supercritical (antidune) waveforms. Results were reviewed by *Allen* [1982]. While the stability analysis clearly is plausible over extant topographic variations, which condition the flow appropriately by causing convective acceleration over the waves, it is not clear, in light of the random nature of spatial and temporal variations in the turbulent velocity profile over rough boundaries, that bed forms can be initiated in this manner [*McLean*, 1990].

[7] There are two distinct problems here. First, by what process are bed forms initiated? Then, given that the inception of a bed form modifies both the boundary and the flow over it, what is their ultimate, stable configuration? In this paper, we essay the first problem. It is clear that bed forms can be propagated from an imposed defect. It is the lack, in the general case, of such an initiating defect that has given rise to the range of hypotheses concerning the effect of turbulent variations in the flow over a labile boundary.

[8] An alternative notion is that, instead of an initial perturbation being impressed onto the bed by turbulent entrainment and deposition of sediment, a transverse instability is generated directly at the sediment-water interface by the interaction of the two deforming media. The idea was introduced by *Bucher* [1919] and was entertained by *von Kármán* [1947]. *Liu* [1957] revisited the idea, envisioning an instability of Kelvin-Helmholtz type at the interface of the sediment-laden wall region and the viscous sublayer of the overlying turbulent flow resulting in a shear layer characterized by periodic streamwise variations in velocity along the bed. However, the measurements necessary to test the idea were beyond the technique of the 1950s. The idea has been revisited since in analytical form by *Moshagen* [1984], who worked on an advanced shear layer K-H instability model, and by *de Jong* [1983, 1985, 1989], who considered bed form initiation by an internal wave instability in flow stratified by velocity and density (related to suspended sediment concentrations). However, direct comparisons of the analytical work with measurements of the mechanisms are still lacking.

[9] The interfacial instability concept has been criticized and discounted on two principal grounds: (1) there is general skepticism among sedimentologists that a granular bed can be regarded as a continuum (in effect, as a fluid), hence that the model is appropriate, and (2) the length scales (quite small) are inappropriate for developed bed forms. Furthermore, the analysis predicts symmetrical features whereas current-directed waveforms are well known to be generally asymmetrical.

[10] Contrary to the first objection, physicists have been accustomed for a long time to deal with slurries as continuous media and there has recently developed a subfield that examines dry grain flows as continua [cf. *Shinbrot*, 1997; *Prasad et al.*, 2000; *Goldfarb et al.*, 2002]. It has even been demonstrated that granular flows conform to Prandtl's
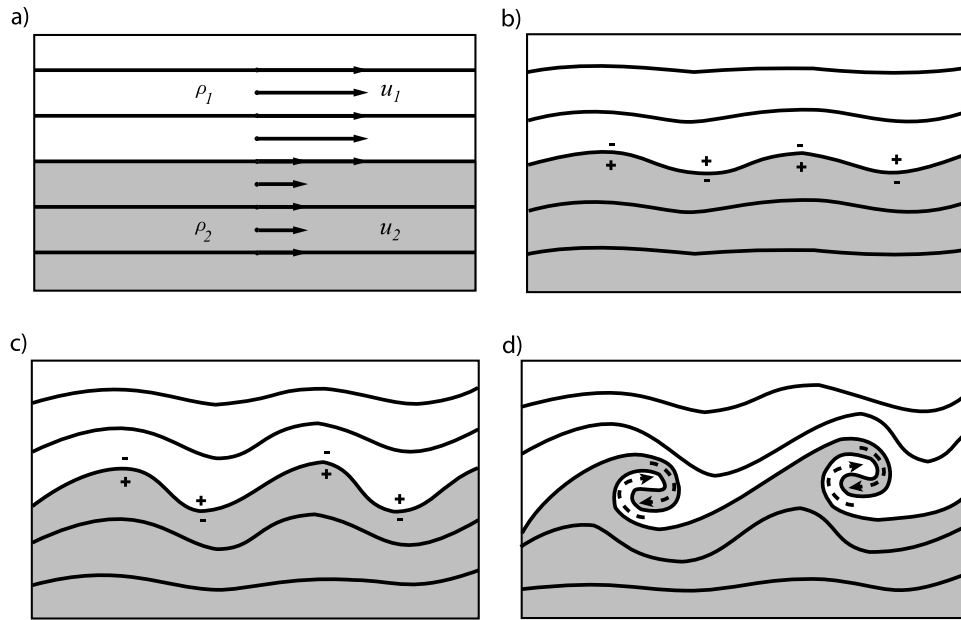
Figure 1. Development of a sheared density interface of Kelvin-Helmholtz type between two fluids when the upper fluid is less dense but faster moving (Figure 1a). Streamwise variation in velocity causes convergence (acceleration) and divergence (deceleration) of streamlines, creating internal waveforms on the interface (Figure 1b). From Bernoulli's principle, a decrease in velocity is counteracted by an increase in pressure, and vice versa. The pressure variations are accentuated with time (Figure 1c), resulting in the concentration of vorticity at the waveform crests and the generation of discrete transverse vortices (Figure 1d). The plus and minus signs in Figures 1b and 1c indicate increased or decreased pressure across the interface. We suppose that the much more highly inertial lower layer retains the imprint of the simple waveforms. After *Rouse* [1946], with permission from Dover Publications.

mixing length hypothesis [*Wang*, 2004] and other well-known instabilities are being identified in granular matter flows [e.g., *Shinbrot et al.*, 1999; *Goldfarb et al.*, 2002; *Conway et al.*, 2004]. For example, *Goldfarb et al.* [2002] have demonstrated that classic "hydrodynamic" shear instabilities can form at the interface between two granular material flows that eventually form breaking waves nearly identical to those depicted in Figure 1. *Conway et al.* [2004] have also identified Taylor-type vortices in granular flows. In general, interfacial effects may be expected between any continuously deforming media with densities not too different than each other. The notion that the disperse slurry of sand and water that constitutes the surface of a deforming sand bed may be viewed as a continuously deforming medium is entirely consistent with experience.

[11] As for the second objection and the caveat about the analysis predicting symmetric bed waves, there is no reason to assume that an instability that gives rise to well-organized variations in sediment transport must continue to dominate the flow once bed waves are established. There is no inconsistency between the idea of bed form initiation by a fluid mechanical instability and bed form growth by wave amplification. Furthermore, the concept of a classical instability offers an explanation for the regularity of transverse bed forms since they are considered to arise from the local mean flow. This line of thought deserves revisitation. Accordingly, the purpose of this paper is to report exploratory experiments designed to investigate the feasibility of a classical fluid mechanical instability as the explanation for the inception of transverse bed forms under unidirectional water flows. We reintroduce a simple quantitative model for

hydrodynamic instability to explain bed form initiation and present the results of our experimental tests of it.

## 2. A Simple Model for Interfacial Instability

[12] *Liu* [1957] recognized that a moving sand bed might be likened to a dense fluid. Drawing on presentations of theory by *Lamb* [1932], *Rouse* [1946], and *Prandtl* [1952], he noted that an interface between two fluids of densities ρ_1 and ρ_2 moving at velocities u_1 and u_2 respectively will be stable if

$$(u_1 - u_2)^2 < gL(\rho_2^2 - \rho_1^2)/(2\pi\rho_1\rho_2) \qquad (1)$$

in which g is the acceleration of gravity and L is a system length scale. If the squared velocity difference exceeds the right-hand side, the surface is unstable and begins to undulate, forming a Kelvin-Helmholtz wave of length L (Figure 1). It has since been appreciated that a variety of hydrodynamic instabilities may develop on a fluid interface within the Richardson number range $-3 \leq Ri \leq 1$ [*Lawrence et al.*, 1991]. The Richardson number is defined by

$$Ri = \Delta\rho g\delta/(\rho_2\Delta u^2) \qquad (2)$$

in which $\Delta\rho$ and Δu are the density and velocity differentials, ρ_2 is the density of the lower, more dense fluid (in our case, the sand transporting layer) and δ is the thickness of the velocity interface. When $Ri < 0.07$, a
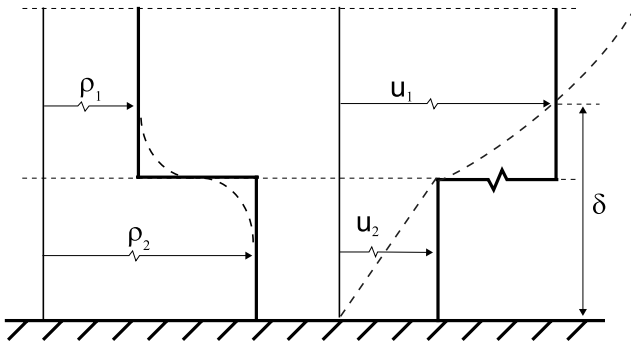
Figure 2. Definition diagram for a two-phase flow of water over a moving sand bed. Solid, rectilinear lines represent the simplified velocity and density profiles of the model, while the dashed lines approximate the real profiles. Here δ gives the thickness of the velocity interface [after *Lawrence et al.*, 1991].

condition commonly satisfied in streamflows over sand beds, the Kelvin-Helmholtz instability dominates. Therefore it is interesting to investigate whether the interface between a water flow and a sand transporting layer is susceptible to this instability.

[13] In the relation represented by equation (1), it is assumed that flow is two-dimensional; both fluids are moving in the same direction; the fluids are inviscid; turbulence is not present or can be ignored; both fluids have infinite depth; and only gravitational forces act on the fluids. These are severe constraints; nonetheless, they are quite familiar assumptions in fluid mechanics as a means to enable analytical solution of problems. Rapid aggradation or degradation of the bed may influence the occurrence of the phenomenon, but equation (1) should hold where slow changes in gradation occur and the bed can be considered in equilibrium over the time frame where the instability occurs. There are some further simplifications in our model (e.g., representing the two flows as "slab flows"; Figure 2) which limit us to the first-order expression given in equation (1). Since our measurements are restricted to quantities that lead to the terms given in equation (1), this represents the best solution that we can presently exploit.

[14] The wavelength at which the interface becomes unstable is extracted from a simple rearrangement of equation (1)

$$L_{K-H} = \frac{2\pi(u_1 - u_2)^2 \rho_1 \rho_2}{g(\rho_2^2 - \rho_1^2)} \qquad (3)$$

Liu [1957] proposed this condition as a viable mechanistic description and explanation for the establishment of transverse sandy bed forms. He supposed the less dense, faster moving layer to be the viscous sublayer and the more dense, slower moving layer to be the mobile sediment layer moving over the bed. The measurements taken during the present study allow a test of the conjecture.

3. Experimental Methods

3.1. Flume Arrangements

[15] Experiments were conducted at the National Sedimentation Laboratory, United States Department of Agri-

culture, in Oxford, Mississippi. A tilting, recirculating flume 1 m wide and 15.2 m long was loaded with 2250 kg of homogeneous, narrowly graded white quartz sand (Ottawa sand; $D_{50} = 0.5$ mm) that had been washed and sieved. Prior to each run, the sand bed was carefully flattened to remove all variations greater than 1 mm in height (Figure 3a). It was then subjected to a 0.15 m deep, unidirectional, nonvarying flow. Bed form development was observed over five separate flow stages that were both subcritical and fully turbulent. Flow conditions are summarized in Table 1. The two lower-flow stages are at or below the threshold for motion for this sediment (nondimensional critical Shields stress $\theta_{cr} = 0.035$ for 0.5 mm sand [*Miller et al.*, 1977]) and plot near the boundary between ripples and dunes on bed form existence diagrams [*Southard and Boguchwal*, 1990]. The three higher flows are well above the threshold for motion and fall squarely within the range in which dune bed forms are predicted to occur [cf. *Venditti et al.*, 2005a]. The experiments are not scaled since the bed material is full size.

[16] The development of the bed was monitored using a high-resolution video camera mounted above the flume 10.3 m from the headbox. The video was focused to capture the width of the flume bed and was illuminated with four 100-W flood lamps mounted on the flume sidewalls and oriented to intersect at the camera focal point. The side lighting produced a glare-free image with shadows that highlighted millimeter-scale changes in the bed structure (see *Venditti et al.* [2005b] for further information). In addition to these runs, another series was conducted to estimate grain velocities in the bed load layer using 0.5 mm black glass seed particles. A 25.4 mm thick Plexiglas plate (0.3 m wide × 0.5 m long) was suspended at the water surface with a beveled upstream edge. The plate surface was illuminated by two 500-W and four 100-W flood lamps such that light penetrated the glass and the view from above was free of distortions caused by the water surface. In these runs, images were captured at a frequency of 30 Hz of an 0.2 × 0.2 m area of the bed.

[17] Changes in bed height were monitored using two acoustic echo sounders mounted in the center of the channel with a streamwise separation of 0.133 m. Bed form heights and lengths, measured from the echo sounder records, and migration rates, calculated by finding the time required for the bed form to pass between the echo sounders, were used to calculate the transport rates associated with the initial sand waves using methods outlined by *Simons et al.* [1965]. We also attempted direct measurements of sand transport rate (which was essentially entirely bed load) using a miniature Helley-Smith sampler.

3.2. Characterization of the Active Layer

[18] Additional properties of the sediment transporting (active) layer could not be measured directly. We require, in particular, its depth and density. Several relations have been presented in the literature (reviewed by *Bridge and Bennett* [1992]) to predict d_{tl}, the depth of the transport saltation layer. *Einstein* [1950] suggested, in his seminal treatise on bed load transport, $d_{tl} \approx 2-3D$. Other relations are based on the assumption that d_{tl} varies with shear stress (or shear velocity). The most frequently cited are those of *Bagnold* [1973], *Bridge and Dominic* [1984], and *van Rijn* [1984], all of which consist of an empirical relation between d_{tl} and some measure of the shear stress above the critical value for
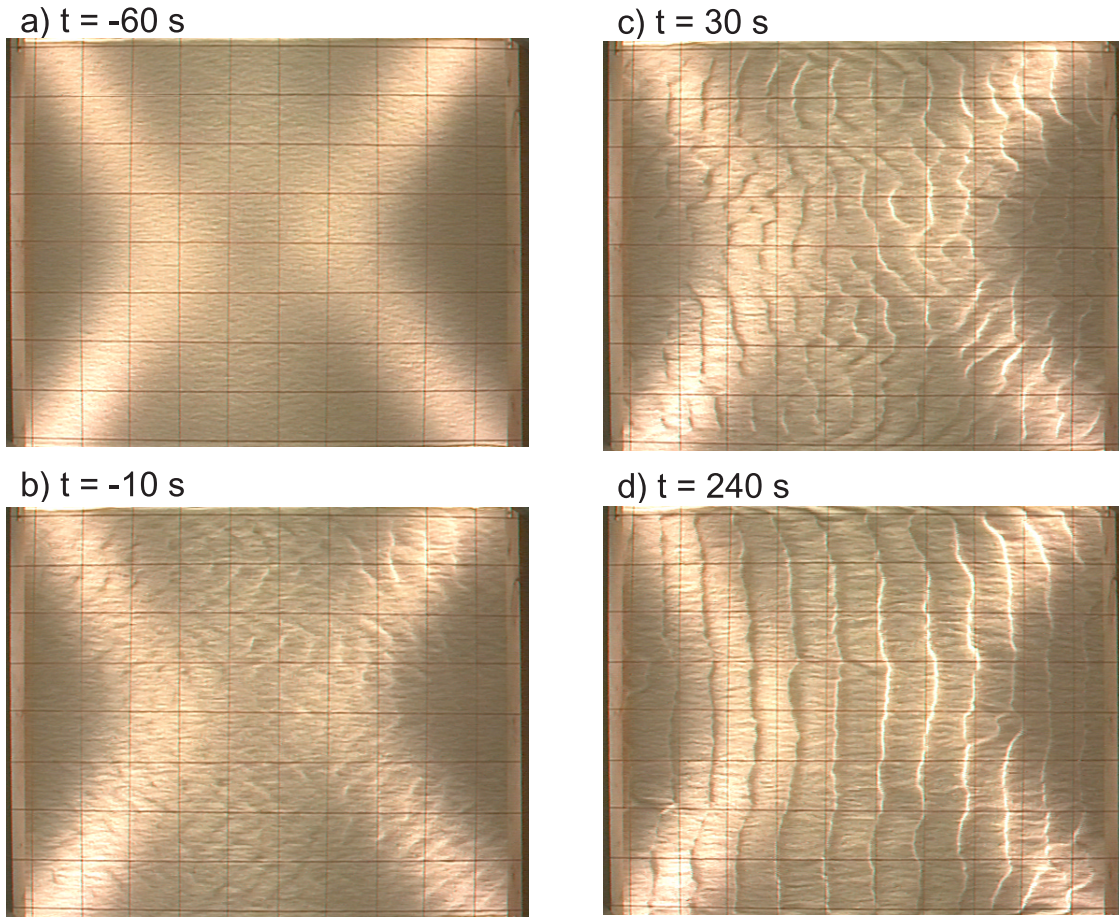
Figure 3. Evolution of a bed form field through instantaneous initiation. Grid spacing is 0.115 m; flow is left to right. Prior to $t = 0$ s, discharge was being ramped up to the desired flow. Mean velocity is 0.50 m s^{-1}; flow depth is 0.15 m; Froude number is 0.41; Reynolds number is 76 000; boundary shear stress, estimated from the law of the wall using the lower 20% of the velocity profile, is 0.90 Pa, which is equivalent to a nondimensional Shields stress (θ) of 0.111. Images are drawn from the high-resolution (super-VHS) video camera.

entrainment. The *Bridge and Dominic* [1984] equation is based on data of *Abbott and Francis* [1977] consisting of observations of the motion of solitary pea gravel particles over a fixed bed of rounded grains with 4.8 mm $\leq D \leq$ 9.6 mm. Bagnold and van Rijn both back-calculated values of d_{tl} from sand transport rates ($D_{50} = 1.35$ mm) measured by *Williams* [1970]. We tested all of these methods for the conditions measured in our experiments, and all estimated values are of order 1 mm. Hence it appears that results generated by any of these relations might reasonably be accepted.

4. Observations

4.1. Phenomena

[19] Two processes of bed form initiation were observed. At the two lower flows, sediment transport remained patchy and sporadic and the flat bed persisted for a long time. However, if a bed defect (a small pit or mound, of height $h \approx$ 8−10 mm; $h/D \approx$ 16−20) and diameter ∼30 mm was introduced artificially, local sediment transport and flow separation propagated the defect downstream and laterally, forming new bed forms in the manner previously described

by others [e.g., *Southard and Dingler*, 1971]. The angle of the lateral propagation was about 12° (i.e., the interior angle of the bed form field was 24°) so that, after a distance of 2.35 m, the bed forms covered the entire width of the bed.

[20] At the three higher flows, sediment transport was general and continuous, and bed form initiation was sensibly instantaneous everywhere on the bed. Artificial defects

Table 1. Summary of Flow Parameters[a]

Flow Parameter	Flow A	Flow B	Flow C	Flow D	Flow E
d, m	0.152	0.152	0.153	0.153	0.153
$\overline{U}$, m s^{-1}	0.501	0.477	0.454	0.399	0.356
$S \times 10^{-4}$	12	11	7.0	5.5	5.5
Fr	0.411	0.391	0.370	0.326	0.290
Re	75936	72331	69568	61093	54580
u_*,[b] m s^{-1}	0.030	0.026	0.022	0.017	0.016
τ,[b] Pa	0.902	0.650	0.481	0.291	0.242
θ[b]	0.111	0.080	0.059	0.036	0.030

[a]Velocity data are derived from measurements taken with a 300-mW Dantec Laser Doppler Anemometer (see *Venditti* [2003] for details). $Fr = \overline{U}/(gd)^{0.5}$, $Re = d\overline{U}/\nu$, $u_* = (\tau/\rho)^{0.5}$, $Re_g = Du_*/\nu$, $\theta = \tau/[gD(\rho_s - \rho_w)]$.
[b]Determinations based on law of the wall using lower 20% of velocity profiles.

Table 2. Observed and Estimated Parameters Used in the Calculation of the Instability Model[a]

Parameter	Flow A	Flow B	Flow C
Surface particle velocity, $\overline{u}_p$,[b] mm s^{-1}	36.6 ± 2.2	34.0 ± 2.5	26.7 ± 2.1
Depth-averaged u_p, mm s^{-1}	18.3 ± 1.1	17.0 ± 1.3	13.3 ± 1.1
Flow velocity at z = 5 mm, $u_{5.0}$,[b] mm s^{-1}	309.2 ± 0.3	295.2 ± 0.3	289.6 ± 0.2
Flow velocity at z = 2.5 mm, $u_{2.5}$,[c] mm s^{-1}	255.9 ± 17.1	258.1 ± 8.0	259.1 ± 13.1
Shear velocity, u_*,[c] mm s^{-1}	29.9 ± 1.4	25.5 ± 0.6	21.8 ± 1.2
Depth of transport layer, d_{tl}, mm	0.99 ± 0.028	0.90 ± 0.014	0.82 ± 0.026
Initial dry-mass transport rate, Q_s,[b] kg s^{-1} × 10^{-3}	7.69 ± 0.51	5.76 ± 0.36	4.38 ± 0.65
Mass of sand in transport layer, M_s, kg × 10^{-3}	7.69 ± 0.51	5.76 ± 0.36	4.38 ± 0.65
Mass of water in transport layer, M_w, kg × 10^{-3}	15.1 ± 1.22	13.1 ± 1.16	9.25 ± 0.96
Volume of active layer, V_{tl}, m^3 × 10^{-5}	1.80 ± 0.12	1.53 ± 0.12	1.09 ± 0.09
Combined density, ρ_{tl}, kg m^{-3}	1265 ± 112	1235 ± 123	1250 ± 151

[a]Error ranges are ±1 standard error.
[b]Directly measured quantities.
[c]Based on a regression in the form $u = m(\ln z) + b$.

were washed away without imposing any observable effect on the bed. The development of the bed from flat to two-dimensional bed forms (in fact, dunes [see *Venditti et al.*, 2005c]) is documented by a series of images extracted from our video record (Figure 3). Initially, the bed was covered with lineated striations, oriented along the flow, with spacing approximately equivalent to the expected streak spacing $\lambda_s = 100\nu/u_*$, wherein ν is kinematic viscosity and u_* is the shear velocity (see *Best* [1992] for a review). The following sequence of deformations was then observed: (1) a cross-hatch pattern is imprinted on the bed, (2) chevron-shaped scallops develop at the nodes of the cross-hatch (Figure 3b) [cf. *Gyr and Schmid*, 1989], (3) the chevrons begin to migrate and organize into incipient crest lines (Figure 3c), (4) the crest lines straighten into two-dimensional features (Figure 3d), and (5) the bed forms grow in height and length.

[21] These developments are described in detail by *Venditti et al.* [2005b]. Two features of the sequence are important in the present context. First, the cross-hatch pattern, ∼1 to 2 D in height, appeared everywhere on the bed and in highly organized fashion within a few seconds. Second, the entire process occurred within 100 s. This represents far too little time for the effects to be transferred along the flume by defect propagation. The initial cross-hatch and chevron features begin to appear during the ramping-up period of the flow, so it is possible that they are associated with the onset of turbulent flow. Nonetheless, they directly give rise to transverse bed forms several grain diameters high and with initial wavelengths averaging 80 to 90 mm.

[22] In the flows investigated, Ri < 0.02, so it appears appropriate to test the hypothesis that the observed initial bed deformation conforms with a Kelvin-Helmholtz instability.
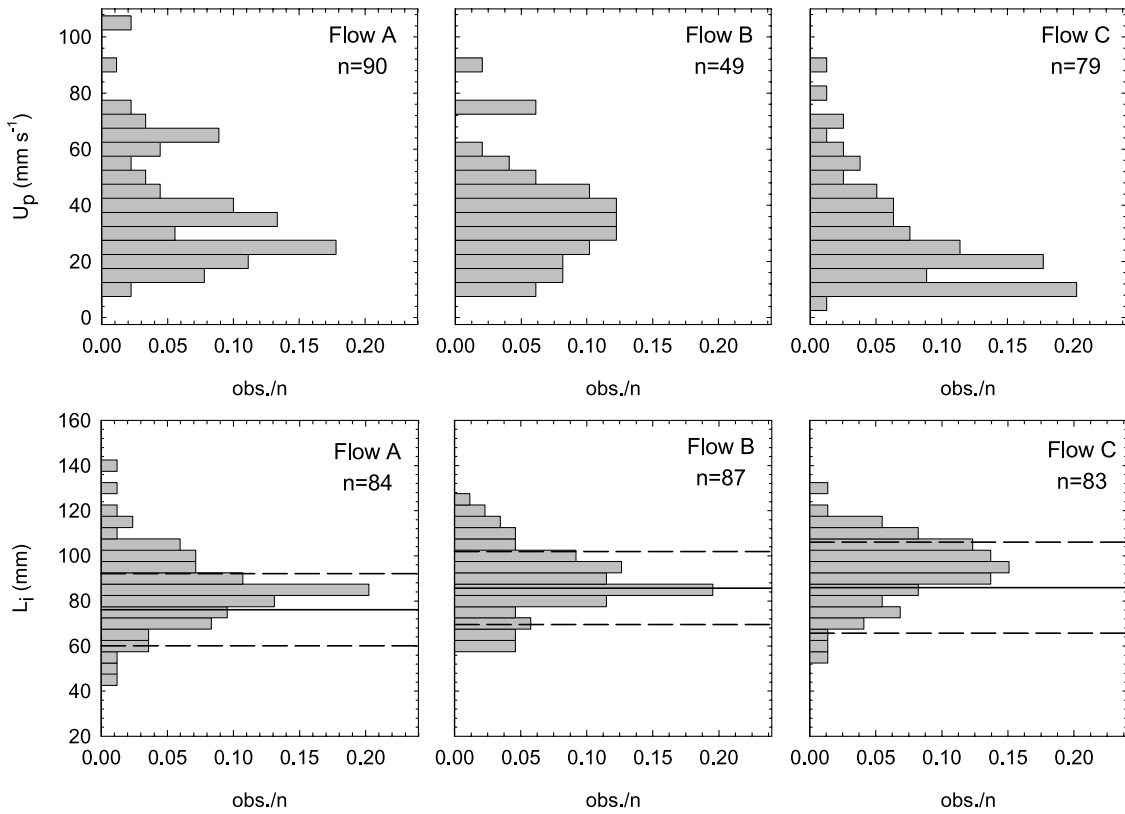
4.2. Measurements

[23] The interfacial instability scenario envisioned herein is slightly different from that considered by *Liu* [1957]. He supposed the viscous sublayer to be the upper fluid, but our flows were hydraulically transitional suggesting a well developed sublayer was absent. Velocities (and associated fluid layers) that might be considered include the water column mean velocity, log layer mean velocity, and buffer zone velocity immediately above the transport layer. At 0.2d (lower 20% of flow depth), the log layer depth in our experiments was 31 mm and the mean velocity would be the actual velocity at 11.2 mm above the bed surface. We

have measurements at 10 mm. Our lowest velocity measurements were made at 2.5 mm (i.e., 5D) above the bed and they were sometimes contaminated by saltating grains, so these measurements certainly represent the velocity immediately above the transport layer. We also have long sequences of measurements at 5 mm above the surface. The measurements at 2.5 mm, $u_{2.5}$, appear to be the most appropriate ones, but we estimated the mean velocity there from the logarithmic profile rather than use the measurements directly because of the difficulty experienced in making the measurements. The data are given in Table 2.

[24] The lower fluid depicted in Figure 2 is considered to be the active sediment transport layer. The velocity of particles at the surface of the transport layer was measured from the video images and found to vary between 0.010 and 0.075 m s^{-1}, depending on the run. As flow strength increased, the mean particle velocity, u_p, increased. The range of measurements is illustrated in Figure 4. If we assume that u_p decreases linearly to zero at some depth, the depth-averaged particle velocity is $u_p/2$ (Table 2). Measurements by *Paulos* [1998] suggest that the u_p profile is, in fact, linear, but the transport layer is so thin that other assumptions would yield estimates not very different. It will turn out, in any case, that the assumption made here is not very critical.

[25] Estimates of the active transport layer depth from the method described above are given in Table 3. We adopt the estimates from Bagnold's method for calculating of the volume of the active layer, V_{tl}. The mass of sediment in V_{tl} is determined from the dry mass transport rate, Q_s, as $M_s = Q_s t$, in which t is a suitable integral period (we choose 1 s for convenience). There are two candidate Q_s values for each run, that measured by the Helley-Smith sampler, Q_{s-HS}, and that determined from the progression of the nascent waveforms, Q_{s-sw}, using the method of *Simons et al.* [1965] (Table 4). There is a large variance associated with Q_{s-HS}, but this is not unexpected since bed load sampler measurements are notoriously variable. Q_{s-sw} is calculated using all bed forms observed during the first 10 min of echo sounding, when bed form height, H, was generally less than 5 mm (transport rate increased significantly after H exceeded 5 mm). Estimates returned by the two methods vary by 30 to 60% (Table 4) but the sand wave measurements, which we regard as the more reliable, show a reasonable increase in transport with flow strength.

Figure 4. Histograms of bed surface particle velocity, u_p, during bed form initiation and initial bed form lengths, L_i. Measurements of u_p were made over 30 s following the onset of widespread sand transport. Measurements of L_i are from images collected just as the 2-D bed form field was established (see *Venditti et al.* [2005a] for further information). Solid lines indicate predicted wavelength using $u_{2.5}$ and $u_p/2$, and the associated error estimates are the dashed lines.

Selection of Q_{s-sw} to represent sediment transport also increases our number of observations, which ultimately reduces the error estimate. The mass of water, M_w, in V_{tl} is $\rho_w(V_{tl} - V_s)$, in which V_s is the volume of sediment grains in the transport layer, calculated as M_s/ρ_s. Using M_s and M_w, the density of the active transport layer is finally calculated as $\rho_{tl} = (M_s + M_w)/V_{tl}$. Table 2 gives the estimates of Q_s, M_s, M_w and ρ_{tl} used in further calculations.

5. Analysis

5.1. Errors

[26] All measured quantities have some associated error. Error analysis followed the rules for propagation of error [e.g., *Beers*, 1957; *Parratt*, 1961] when a quantity was derived from multiple measured quantities. Standard errors of estimate are presented in Tables 2 and 4 as two standard error ranges ($2\sigma/\sqrt{n}$) for each parameter.

[27] The error associated with d_{tl} is derived from the error associated with the least squares regression (of the velocity profile) used to determine u_*. The standard error of u_* varies between 5.0% and 10.6% of the measurements, which leads to errors of 3.0–6.4% for d_{tl} as estimated from Bagnold's formula. The values are reduced below the error for u_* because of the fractional power in the formula.

[28] The error associated with $u_{2.5}$, the upper layer representative velocity, is 6.2–13.3%. There is, in addition, the question of possible bias that would arise if the selected upper layer velocity is not the most appropriate one. We deal with this matter by presenting comparative calculations

Table 3. Estimates of Transport Layer Depth, d_{tl}[a]

Source	Estimate	Flow A	Flow B	Flow C
Einstein [1950]	$d_{tl} = 2 - 3D$	1.0–1.5	1.0–1.5	1.0–1.5
Bagnold [1973]	$d_{tl} = 1.4(u_*/u_{*cr})^{0.6}D$	0.99	0.90	0.82
Bridge and Dominic [1984]	$d_{tl} = c\,[2.53(\theta - \theta_{cr})^{0.5} + 1]D$	0.85	0.77	0.69
van Rijn [1984]	$d_{tl} = 0.3D_*^{0.7}T^{0.5}D$	1.29	1.00	0.73

[a]The *Bridge and Dominic* [1984] relation is a version from *Bridge and Bennett* [1992] that has been modified such that $d_{tl} \approx D \approx k_s$ at the threshold of motion (k_s is the roughness height and c is a constant ≈ 1). Subscript cr represents critical values for the entrainment of sediment from the Inman curve of *Miller et al.* [1977]. In the van Rijn relation, $D_* = D[g(\rho_s/\rho_w - 1)/\nu^2]^{1/3}$, $T = (\tau - \tau_{cr})/\tau_{cr}$, and τ represents the local shear stress as determined from the log layer velocity profile. Values are in mm.

Table 4. Sediment Transport Estimates[a]

Flow	Helley-Smith Samples		Sand Wave Translation	
	n	$\overline{Q}_{s-HS}$, kg hr^{-1}	n	$\overline{Q}_{s-sw}$, kg hr^{-1}
A	1	18.12	21	27.69 ± 1.84
B	1	33.28	17	20.74 ± 1.29
C	2	11.04 ± 2.46	9	15.76 ± 2.35

[a]Helley-Smith samples were taken over a flat bed, a condition that lasted for varying periods of time. The sand wave translation estimate is for all bed forms observed in the first 10 min of the experiment. Sand waves varied from 1.5 to 8 mm in height during this period, roughly increasing with time. After this 10 min period, there is a dramatic increase in the sand wave size.

for $u_{5.0}$, for which we have long series of measurements that reduce the measurement error to negligible proportions.

[29] The error of ρ_{tl} is considerably greater, varying from 18 to 24% as this calculation compounds errors associated with V_{tl}, M_s and M_w. The bulk of the error associated with V_{tl} is derived from the measurements of u_p, which has associated proportional errors of 12–16%. The error associated with M_s is also large and entirely derived from the error associated with Q_s; 13% (flows A) 12% (flow B) to 30% (flow C). The large error in the latter case is the direct consequence of the small number of observations. Since M_w is calculated as a function of V_{tl} and V_s ($\propto M_s$), its error is also large.

[30] Application of equation (3) compounds these errors, resulting in a relatively large error for the estimates of L_{K-H}, in the range 37–47%. Nearly all the error is associated with the estimates of Q_s and u_p. The error of Q_s could be reduced by substantially increasing the numbers of samples taken but, for u_p, an improved technique is required.

[31] In comparison with the errors associated with the predicted wavelength, the error associated with the observed bed form lengths (Table 5) is in the range 3.5–4.4%, which implies that these values are well known.

5.2. Comparison

[32] Table 5 summarizes observed mean wavelengths of the initial 2-D bed forms in each of the three experimental runs which produced spontaneous bed deformation and presents several predictions based on equation (3). The preferred comparison is for $u_{2.5}$ and $u_p/2$, since these incorporate the best characterization of the velocity change across the interface between the water flow and the active bed layer. While the predictions have substantial associated ranges of uncertainty, the actual values all fall within 10% of the observed values.

[33] Predictions employing $u_{5.0}$, on the other hand, vary significantly from the observations, there being overlap of the error ranges only for flow C, despite the large error margins associated with the predictions. Recognizing that the transport layer is very thin and that u_p cannot be well characterized beyond the surface measurements, we also computed L_{K-H} for $u_{2.5}$ and u_p. Predictions were lower, than the observed distributions reflecting the smaller difference between the upper and lower velocities in this case, but the prediction was significantly low only for flow A.

6. Concluding Discussion

[34] Recent experimental results suggest there are at least two distinct bed form initiation processes. When the im-

posed flow is near or below the critical shear stress for sediment entrainment and sediment transport is patchy and sporadic, bed forms may be generated from amplifying bed perturbations (local bed defects that are propagated down and across stream by flow separation processes). Alternatively, when the critical shear stress for sediment entrainment is well exceeded, bed form development may occur over the whole bed at once (see *Venditti et al.* [2005b] for further details). The model we test herein is strictly applicable to the latter type if bed form initiation.

[35] Our results are consistent with the hypothesis that transverse waveforms on sand beds sheared by subcritical unidirectional currents are initiated as an interfacial hydrodynamic instability of Kelvin-Helmholtz type when the current is sufficiently vigorous to produce general sediment movement, that is, to create a sediment transport layer that acts as a continuous medium. This result suggests that the instantaneous initiation of bed forms is controlled by a simple hydrodynamic instability. It furthermore appears that a turbulent mechanism need not be invoked [cf. *Kuru et al.*, 1995; *Coleman and Eling*, 2000]. This outcome is in contrast to theories of bed form initiation based on the notion that coherent turbulent eddy structures alone imprint an organized pattern of waveforms on the bed, but it is consistent with the observed high degree of regularity of the observed forms. Coherent vortices are certainly the mechanism by which sediment is mobilized and maintained in transport. Here we maintain that the instability is the mechanism that provides order to the transport system.

[36] The instability creates localized erosion and deposition of sediment to produce migrating sedimentary features. The waveforms that arise are scaled to the heights of both fluid layers, which is consistent with the idea that there is mixing of the upper fluid into the lower fluid and visa versa (Figure 1). The bed forms, however, have much greater inertia than the overlying water flow so that they persist and, in turn, impress themselves onto the flow. The subsequent growth and development of the bed forms does not preserve the initial K-H scaling. In fact, the features grow to very much larger equilibrium dimensions which appear, rather, to scale with the entire boundary layer flow over them (or with flow depth when the boundary layer thickness is constrained, as in most rivers) [*Yalin*, 1964, 1992].

[37] It is interesting that our further observations suggest that, once K-H scales are exceeded, the waveforms readily break up into the familiar 3-D features [see *Venditti et al.*, 2005a] that are created ab initio in cases of finite bed perturbation. At this stage, perturbation theories of wave-

Table 5. Comparison of Observed With Predicted Bed Form Wavelengths

Waveform	Flow A	Flow B	Flow C
Observed initial wavelength, mm	82.7 ± 1.8	85.6 ± 1.5	90.8 ± 1.6
Predicted wavelength, $u_{2.5}$, $u_p/2$, mm	76.1 ± 16.0	87.5 ± 16.2	85.9 ± 20.2
Ratio, predicted/observed	0.92	1.02	0.95
Predicted wavelength, $u_{5.0}$, $u_p/2$, mm	114 ± 17.4	116 ± 20.1	109 ± 22.7
Predicted wavelength, $u_{2.5}$, u_p,[a] mm	64.8 ± 14.1	75.6 ± 14.1	76.8 ± 18.2

[a]Note volume of the transport layer is $V_{tl} = d_{tl}\, y_w\, u_p/2$ even though u_p is not halved in equation (3).

form growth and equilibrium quite plausibly apply to the features. In fact, in their recent analytic examination of bed form growth from a flat sand bed, *Zhou and Mendoza* [2005] explicitly decouple the initial sand wave development and subsequent growth toward equilibrium. They suggest the latter phase begins once the height of the initial forms exceeds the viscous sublayer and that the initial phase is skipped when the sublayer is absent. Our observations during the experiments would suggest the decoupling occurs when the bed forms are of sufficient height and asymmetry to initiate strong coherent flow separation cells.

[38] It has been argued that initial bed form lengths measured at laboratory scales are insensitive to variation in fluid shear stress and, instead, scale with grain size [*Coleman and Melville*, 1996]. This argument is consistent with the K-H model in so far as ρ_2 is controlled by the near bed sediment concentration, which is know to reach a maximum of $\sim$30% across a wide range of shear stresses [e.g., *Sumer et al.*, 1996].

[39] Our measurements and the comparison with theory represents only a preliminary exercise to test the theory of hydrodynamic instability in the context of bed surface waveforms. We have not tested a wide range of flows, although our flows fall squarely within the range in which dune bed forms are predicted to occur, and we have studied only a single, narrowly graded sand. We do not know what happens when significant sediment suspension occurs (but we do know that sensibly identical transverse waveforms grow in this circumstance in nature). Our theoretical results derive only from a first-order solution of the hydrodynamic problem. A more advanced solution will take into account the velocity profiles in the near-bed region and through the active layer. In comparison with the requirements of the problem, our measurements also remain rather crude. In particular, the solution is sensitive to the actual bed load transport, which determines the density of the active layer. Indeed, this relation may very well control the hydraulic range within which subcritical transverse waveforms can develop. Unfortunately, bed load transport remains the most difficult condition to measure in the short term, at a point.

[40] We nevertheless assert that our results are sufficient to indicate that a hydrodynamic interfacial instability between the water flow and the labile sand bed is capable of forming organized transverse bed forms in unidirectional water flows.

Notation

b, m	regression intercept and slope.
d	flow depth.
d_{tl}	depth of transport layer.
D_*, T	van Rijn's normalized grain size and shear stress (transport stage).
D, D_{50}	grain size and its median value.
g	gravitational acceleration.
h	defect height.
L	flow system length scale.
L_i	bed form length and its initial value.
L_{K-H}	wavelength of a Kelvin Helmholtz instability.
M_w, M_s	mass of water and sediment in the transport layer.
n	number of observations.
Q_s	sediment flux.
Ri	Richardson number.
t	time.
$u, u_{2.5}, u_{5.0}$	streamwise velocity and its value at 2.5 and 5.0 mm above the bed.
u_*, u_{*cr}	shear velocity and its critical value for sediment entrainment.
u_1, u_2	velocity of upper and lower layers in the K-H model.
u_p	surface particle velocity.
V_s	volume of sediment in the transport layer.
V_{tl}	volume of the transport layer.
y_w	channel width.
z	height above the bed.
δ	thickness of velocity interface.
λ_s	streak spacing.
ρ_1, ρ_2	density of upper and lower layers in the K-H model.
ρ_{tl}	density of the transport layer.
ρ_w, ρ_s	density of water and sediment.
σ	standard deviation.
τ, τ_{cr}	shear stress and its critical value for sediment entrainment.
θ, θ_{cr}	Shields stress and its critical value for sediment entrainment.
v	kinematic viscosity.

References

Abbott, J. E., and R. D. Francis (1977), Saltation and suspension trajectories of solid grains in a water stream, *Proc. R. Soc. London, Ser. A*, *284*, 225–254.

Allen, J. R. L. (1982), *Sedimentary Structures: Their Character and Physical Basis*, Elsevier, New York.

Ashley, G. M. (1990), Classification of large-scale subaqueous bedforms: A new look at an old problem, *J. Sediment. Petrol.*, *60*, 160–172.

Anderson, A. G. (1953), The characteristics of sediment waves formed on open channels, paper presented at the 3rd Mid-western Conference on Fluid Mechanics, Univ. of Missouri, Missoula.

Ashworth, P. J., S. J. Bennett, J. L. Best, and S. J. McLelland (1996), Coherent flow structures in open channels, John Wiley, Hoboken, N. J.

Bagnold, R. A. (1935), The movement of desert sand, *Geogr. J.*, *85*, 342–365.

Bagnold, R. A. (1956), Flow of cohesionless grains in fluids, *Philos. Trans. R. Soc. London, Ser. A*, *249*, 235–297.

Bagnold, R. A. (1973), The nature of saltation and bed-load transport in water, *Proc. R. Soc. London*, *332*, 473–504.

Beers, Y. (1957), *Introduction to the Theory of Error*, Addison-Wesley, Boston, Mass.

Best, J. L. (1992), On the entrainment of sediment and initiation of bed defects: Insights from recent development within turbulent boundary layer research, *Sedimentology*, *39*, 797–811.

Bridge, J. S., and S. J. Bennett (1992), A model for the entrainment and transport of sediment grains of mixed sizes, shapes and densities, *Water Resour. Res.*, *28*, 337–363.

Bridge, J. S., and D. F. Dominic (1984), Bedload grain velocities and sediment transport rates, *Water Resour. Res.*, *20*, 476–790.

Bucher, W. H. (1919), On ripples and related sedimentary surface forms and their paleogeographic interpretation, *Am. J. Sci.*, *47*, 149–210, 241–269.

Coleman, S. E., and B. Eling (2000), Sand wavelets in laminar open-channel flows, *J. Hydraul. Res.*, *38*, 331–338.

Coleman, S. E., and B. W. Melville (1996), Initiation of bedforms on a flat sand bed, *J. Hydraul. Eng.*, *122*, 301–310.

Conway, S. L., T. Shinbrot, and B. J. Glasser (2004), A Taylor vortex analogy in granular flows, *Nature*, *431*, 433–437.

Costello, W. R. (1974), Development of bed configurations in coarse sands, Ph.D. thesis, Mass. Inst. of Technol., Cambridge, Mass.

de Jong, B. (1983), The formation of dunes in open channel flow on a initially flattened erodible bed, in *Proceedings of Euromech 156: Mechanics of Sediment Transport*, edited by B. M. Sumer and A. Müller, pp. 119–126, A. A. Balkema, Brookfield, Vt.

de Jong, B. (1985), The interaction of suspended flow with the bed shape in an open channel, *Proceedings of Euromech 192: Transport of Suspended Solids in Open Channels*, W. Bechteler, pp. 145–154, A. A. Balkema, Brookfield, Vt.

de Jong, B. (1989), Bed waves generated by internal waves in alluvial channels, *J. Hydraul. Eng.*, *115*, 801–817.

Einstein, H. A. (1950), *The Bed-Load Function for Sediment Transportation in Open Channel Flows*, U.S. Dep. of Agric., Washington, D. C.

Engelund, F. (1970), Instability in erodible channels, *J. Fluid Mech.*, *42*, 225–244.

Fredsøe, J. (1974), On the development of dunes in erodible channels, *J. Fluid Mech.*, *64*, 1–16.

Goldfarb, D. J., B. J. Glasser, and T. Shinbrot (2002), Shear instabilities in granular flows, *Nature*, *415*, 302–305.

Grass, A. J. (1970), Initial instability of fine sand, *J. Hydraul. Div. Am. Soc. Civ. Eng.*, *96*, 619–632.

Gyr, A., and A. Schmid (1989), The different ripple formation mechanism, *J. Hydraul. Res.*, *27*, 61–74.

Kennedy, J. F. (1963), The mechanics of dunes and anti-dunes in erodible channels, *J. Fluid Mech.*, *164*, 521–544.

Kennedy, J. F. (1969), The formation of sediment ripples, dunes and anti-dunes, *Annu. Rev. Fluid Mech.*, *1*, 147–168.

Kim, H. T., S. J. W. Kline, and W. C. Reynolds (1971), The production of turbulence near a smooth wall in a turbulent boundary layer, *J. Fluid Mech.*, *50*, 133–160.

Klebanoff, P. S. (1955), Characteristics of turbulence in a boundary layer with zero pressure gradient, *NACA Rep. 1247*, NASA, Washington, D. C.

Kline, S. J. W., W. C. Reynolds, F. A. Schraub, and P. W. Rundstadler (1967), The structure of turbulent boundary layers, *J. Fluid Mech.*, *30*, 741–773.

Kuru, W. C., D. T. Leighton, and M. J. McCready (1995), Formation of waves on a horizontal erodible bed of particles, *Int. J. Multiphase Flow*, *12*, 1123–1140.

Lamb, H. (1932), *Hydrodynamics*, Dover, Mineola, N. Y.

Langbein, W. B., and L. B. Leopold (1968), River channel bars and dunes—Theory of kinematic waves, *U.S. Geol. Surv. Prof. Pap.*, *422–L*.

Laufer, J. (1951), Investigation of turbulent flow in a two-dimensional channel, *NACA Rep. 1053*, NASA, Washington, D. C.

Lawrence, G. A., F. K. Brownand, and L. G. Redekopp (1991), Stability of a sheared density interface, *Phys. Fluids A*, *3*, 2360–2370.

Leeder, M. R. (1980), On the stability of lower stage plane beds and the absence of ripples in coarse sand, *J. Geol. Soc. London*, *137*, 423–429.

Leliavsky, S. (1955), *An Introduction to Fluvial Hydraulics*, Constable, London.

Lighthill, M. J., and G. B. Witham (1955a), On kinematic waves: I. Flood movement in long rivers, *Proc. R. Soc. London, Ser. A*, *229*, 281–316.

Lighthill, M. J., and G. B. Witham (1955b), On kinematic waves II: A theory of traffic flow on long crowded roads, *Proc. R. Soc. London, Ser. A*, *229*, 317–345.

Liu, H.-K. (1957), Mechanics of sediment-ripple formation, *J. Hydraul. Div. Am. Soc. Civ. Eng.*, *83*, 1–23.

McLean, S. R. (1990), The stability of ripples and dunes, *Earth Sci. Rev.*, *29*, 131–144.

Miller, M. C., I. N. McCave, and P. D. Komar (1977), Threshold of sediment motion under unidirectional currents, *Sedimentology*, *24*, 507–527.

Moshagen, H. (1984), Sand waves in free surface flow—A study with emphasis on hydrodynamic effects, Ph.D. thesis, Univ. of Trondheim, Trondheim, Norway.

Nezu, I., and H. Nakagawa (1993), *Turbulence in Open Channel Flows*, A. A. Balkema, Brookfield, Vt.

Parker, G. (1975), Sediment interia as the cause of river antidunes, *J. Hydraul. Div. Am. Soc. Civ. Eng.*, *101*, 211–221.

Parratt, L. G. (1961), *Probability and Experimental Errors in Science*, John Wiley, Hoboken, N. J.

Paulos, Y. K. (1998), Intense bedload transport in non-uniform flow, Ph.D. thesis, Univ. of B. C., Vancouver, B. C., Canada.

Prandtl, L. (1952), *Fluid Dynamics*, Macmillan, New York.

Prasad, S., D. Pal, and M. J. M. Römkens (2000), Wave formations on shallow layer of flowing grains, *J. Fluid Mech.*, *413*, 89–110.

Rathbun, R. E., and H. P. Guy (1967), Measurement of hydraulic and sediment transport variables in a small recirculating flume, *Water Resour. Res.*, *3*, 107–122.

Raudkivi, A. J. (1963), Study of sediment ripple formation, *J. Hydraul. Div. Am. Soc. Civ. Eng.*, *89*, 15–33.

Raudkivi, A. J. (1966), Bedforms in alluvial channels, *J. Fluid Mech.*, *26*, 507–514.

Raudkivi, A. J. (1997), Ripples on a streambed, *J. Hydraul. Eng.*, *123*, 58–64.

Reynolds, A. J. (1965), Waves on the erodible bed of an open channel, *J. Fluid Mech.*, *22*, 113–133.

Richards, K. J. (1980), The formation of ripples and dunes on an erodible bed, *J. Fluid Mech.*, *99*, 597–618.

Rouse, H. (1946), *Elementary Fluid Mechanics*, John Wiley, Hoboken, N. J.

Shinbrot, T. (1997), Competition between randomizing impacts and inelastic collisions in granular pattern formation, *Nature*, *389*, 574–576.

Shinbrot, T., A. Alexander, and F. J. Muzzio (1999), Spontaneous chaotic granular mixing, *Nature*, *397*, 675–678.

Simons, D. B., E. V. Richardson, and C. F. Nordin (1965), Bedload equation for ripples and dunes, *U.S. Geol. Surv. Prof. Pap.*, *462-H*, 9 pp.

Smith, J. D. (1970), Stability of a sand bed subjected to a shear flow of low Froude number, *J. Geophys. Res.*, *75*, 5928–5940.

Southard, J. B., and L. A. Boguchwal (1990), Bed configurations in steady unidirectional water flow, part 2. Synthesis of flume data, *J. Sediment. Petrol.*, *60*, 658–679.

Southard, J. B., and J. R. Dingler (1971), Flume study of ripple propagation behind mounds on flat sand beds, *Sedimentology*, *16*, 251–263.

Sumer, B. M., A. Kozakiewicz, J. Fredsoe, and R. Deigaard (1996), Velocity and concentration profiles in sheet-flow layer of movable bed, *J. Hydraul. Eng.*, *122*, 549–558.

U.S. Army Corps of Engineers (1935), Studies of river bed materials and their movement with special reference to the lower Mississippi River, *Pap. 17*, U.S. Waterw. Exp. Stn., Vicksburg, Miss.

van Rijn, L. C. (1984), Sediment transport, part III: Bed forms and alluvial roughness, *J. Hydraul. Eng.*, *110*, 1733–1754.

Venditti, J. G. (2003), The initiation and development of sand dunes in river channels, Ph.D. thesis, Univ. of B. C., Vancouver, B. C., Canada.

Venditti, J. G., M. Church, and S. J. Bennett (2005a), On the transition between 2D and 3D dunes, *Sedimentology*, *52*, 1343–1359, doi:10.1111/j.1365-3091.2005.00748.x.

Venditti, J. G., M. Church, and S. J. Bennett (2005b), Bed form initiation from a flat sand bed, *J. Geophys. Res.*, *110*, F01009, doi:10.1029/2004JF000149.

Venditti, J. G., M. Church, and S. J. Bennett (2005c), Morphodynamics of small-scale superimposed sand waves over migrating dune bed forms, *Water Resour. Res.*, *41*, W10423, doi:10.1029/2004WR003461.

von Kármán, T. (1947), Sand ripples in the desert, *Technion Yearb.*, *6*, 52–54.

Wang, Z.-T. (2004), A note on the velocity of granular flow down a bumpy inclined plane, *Granular Matter*, *6*, 67–69, doi:10.1007/s10035-004-0158-x.

Williams, G. P. (1970), Flume width and water depth effects in sediment transport experiments, *U.S. Geol. Surv. Prof. Pap.*, *562-H*, 37 pp.

Williams, P. B., and P. H. Kemp (1971), Initiation of ripples on a flat sand bed, *J. Hydraul. Div. Am. Soc. Civ. Eng.*, *97*, 505–522.

Yalin, M. S. (1964), Geometrical properties of sand waves, *J. Hydraul. Div. Am. Soc. Civ. Eng.*, *90*, 105–109.

Yalin, M. S. (1992), *River Mechanics*, Elsevier, New York.

Zhou, D., and C. Mendoza (2005), Growth model for sand wavelets, *J. Hydraul. Eng.*, *131*, 866–876, doi:10.1061/ASCE0733-94292005131:10866.

————————————

S. J. Bennett, Department of Geography, 112 Wilkeson Quad, State University of New York at Buffalo, Buffalo, NY 14261-0055, USA.

M. Church, Department of Geography, University of British Columbia, Vancouver, British Columbia, Canada V6T 1Z2.

J. G. Venditti, Department of Earth and Planetary Sciences, 307 McCone Hall, University of California, Berkeley, CA 94720-4767, USA. (jgvenditti@yahoo.ca)